IR Intra-pixel Sensitivity Variance

C. Pavlovsky, P. McCullough, S. Baggett
December 01, 2011

ABSTRACT

In order to characterize the intrapixel sensitivity variance of the WFC3 IR array, we analyzed full frame IR observations of a star field in Omega Centauri in 2 bandpasses (F110W and F160W) and a star field in 47 Tucanae in 1 bandpass (F160W). To within the measurement error, and independent of wavelength, magnitude bin, or amp, we do not detect any Intra-pixel Sensitivity Variation, IPSV.

Introduction

The response of a detector to incident light may show variations in the total flux detected depending on where the center of the point spread function (PSF) lands within the pixel, an effect known as "intra-pixel sensitivity variance" (IPSV). In such cases, frequently the corners of the pixel measure less flux than the center of pixel; when this happens, it can degrade photometric and astrometric measurements. Previous analysis (Lauer 1999) has shown that IPSV affected both the WFPC2 and NIC3 cameras on HST: the integrated flux was found to vary by a few percent as a function of fractional column position in WFPC2 and by up to +/- 20% in NIC3. Lauer measured the IPSV by first generating a well-sampled PSF (an "effective" PSF) from a dithered dataset using an optimal dither pattern (a regular NxN grid with 1/N subpixel steps). This effective PSF was then shifted and coarsely resampled to simulate the undersampled image. The flux in the interpolated but undersampled PSF could then be directly compared to the effective PSF in order to quantify the IPSV. We will use the same optimal dither pattern, but solve for the IPSV using a matrix analysis technique.

IPSV in the WFC3 IR detector was measured pre-flight during Thermal Vacuum 3 testing (TV3) using the WFC3 optical stimulus (CASTLE) (ISR 2008-29). In the TV3 tests, a single point source-like image at 1050 nm was scanned across the IR detector. The resulting set of ~200 observations, with photometric rms of ~0.6%, showed no measurable IPSV. There was a marginally-significant (3-sigma) dependence of flux on radius from the center of the PSF, but the slope was opposite to that expected based on predictions from gap simulations. The simulation was performed to test the instrument's adherence to the requirement that inter-pixel gaps not exceed 5% of the pixel width, where gap is defined as the region where the flux has dropped to <50% that of the center of the pixel. This Cycle 17 program was designed to increase the measurement precision over that of the TV3 test.

Data

In this Cycle 17 program 11916 data were taken in two filters, F110W and F160W, in full-frame mode, each with a 2x2 subpixel dither box, on a star field in Omega Centauri. The field was chosen to be suitable for precision aperture photometry of hundreds of stars per amplifier; the large number of sources would allow for an improved measure of the IPSV or better constraints if none were measured. The effective IPSV depends on the width of the PSF in pixel units, so two disparate wavelengths (filters F110W and F160W) were desirable, since the FWHM of the PSF will scale with wavelength. We used a 2x2 grid for the dither pattern with 1/2 pixel shifts in X and Y on the grid, based upon the NxN optimal spacing recommended by to Lauer (1999); this was implemented in APT as a BOX pattern with npts=4.

Table 1. Omega Centauri data in F110W and F160W

filename	date-obs	time-obs	subtype	filt	samp_seq	nsamp	exptime (s)
ibc201h8q_flt	2010-01-23	21:17:06	FULLIMAG	F110W	SPARS25	14	302.9
ibc201h9q_flt	2010-01-23	21:23:11	FULLIMAG	F110W	SPARS25	14	302.9
ibc201hbq_flt	2010-01-23	21:29:16	FULLIMAG	F110W	SPARS25	14	302.9
ibc201hdq_flt	2010-01-23	21:35:21	FULLIMAG	F110W	SPARS25	14	302.9
ibc201hfq_flt	2010-01-23	21:41:26	FULLIMAG	F160W	SPARS25	15	327.9
ibc201hhq_flt	2010-01-23	21:47:56	FULLIMAG	F160W	SPARS25	15	327.9
ibc201hjq_flt	2010-01-23	21:54:26	FULLIMAG	F160W	SPARS25	15	327.9
ibc201hlq_flt	2010-01-23	22:00:56	FULLIMAG	F160W	SPARS25	15	327.9

For comparison purposes the archive was searched for additional data with similar characteristics as the dedicated IPSV data. No data taken with the optimal dither pattern in a regular NxN grid of 1/N subpixel steps were found. However, program 11931 did have data from a star field in 47 Tucanae taken with POSTARGS equivalent to a box pattern with a 4.4 pixel shift in one direction and 2.808 pixels in the other. Though not

optimal, since the data met the other requirements of source density and filter, it was included in the analysis here for comparison purposes.

Table 2. 47 Tucanae F160W data

filename	date-obs	time-obs	subtype	filter	samp_seq	nsamp	Postarg1	Postarg2
ibbw04d5q_flt	2010-03-13	17:30:54	FULLIMAG	F160W	SPARS10	11	0.000	0.000
ibbw04daq_flt	2010-03-13	18:11:44	FULLIMAG	F160W	SPARS10	11	0.572	0.000
ibbw04dcq_flt	2010-03-13	19:01:22	FULLIMAG	F160W	SPARS10	11	0.572	0.365
ibbw04dhq_flt	2010-03-13	19:16:25	FULLIMAG	F160W	SPARS10	11	0.000	0.365

Analysis

Photometry

The Omega Centauri star field (Figure 1) was selected to be dense enough to provide photometry of ~2500 stars, but not so dense that aperture photometry would be compromised by the blending of stars. Some blending is acceptable, because we do not need accurate photometry, but instead need precise (relative) photometry of a star compared to dithered versions of itself.

Figure 1. Omega Centauri star field in F160W
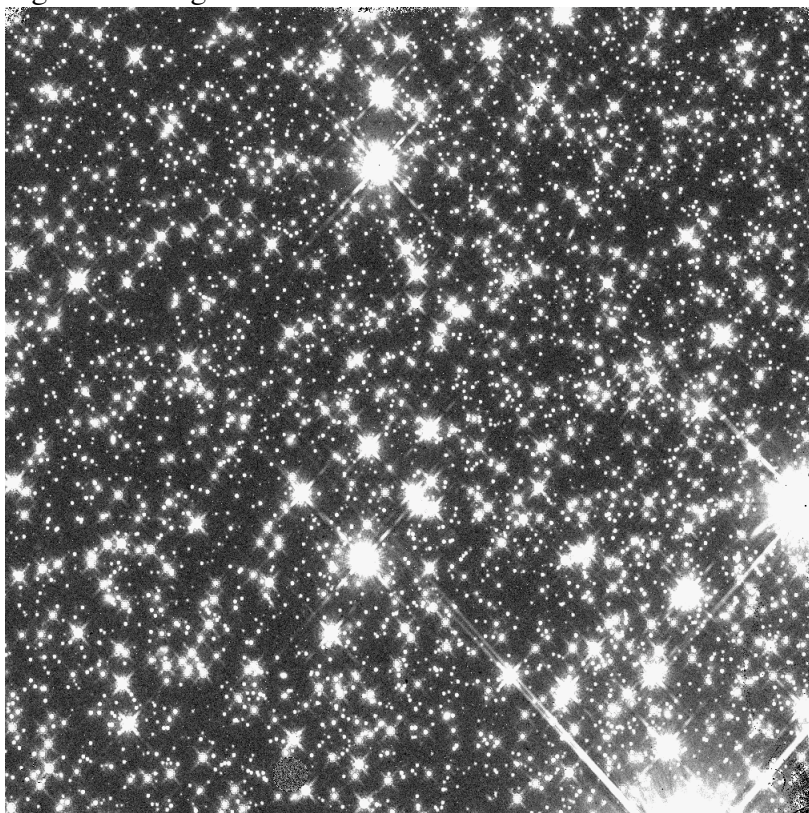
For example, if a star has an unresolved companion that is 10% as bright and separated by 0.1 pixel, the resulting aperture photometry (e.g. for an HR diagram) will be inaccurate at 10%, but the centroid will only be inaccurate at 1% of a pixel, so we expect the effect of stellar blending on IPSV estimates to be of "second order." The star field in 47 Tucanae (Figure 2) also meets these density requirements. Furthermore, most stars will not be blended and by their greater numbers will dominate the least-squares solutions to the over-constrained set of equations that determine the IPSV.

There were approximately 2500 usable stars in each of the three fields. We performed aperture photometry on the pipeline-calibrated files (FLTs) using a 5 pixel radius and a sky annulus from 7 to 9 pixels. Sources were preselected using starfind in IRAF. Initial photometry was done with these lists using qphot in IRAF. The resulting photometry files were scrubbed for sources that were within 12 pixels of each other, detections of bad pixels, etc. Then the photometry with qphot was repeated on the cleaned lists.

Figure 2. 47 Tuncanae star field in F160W
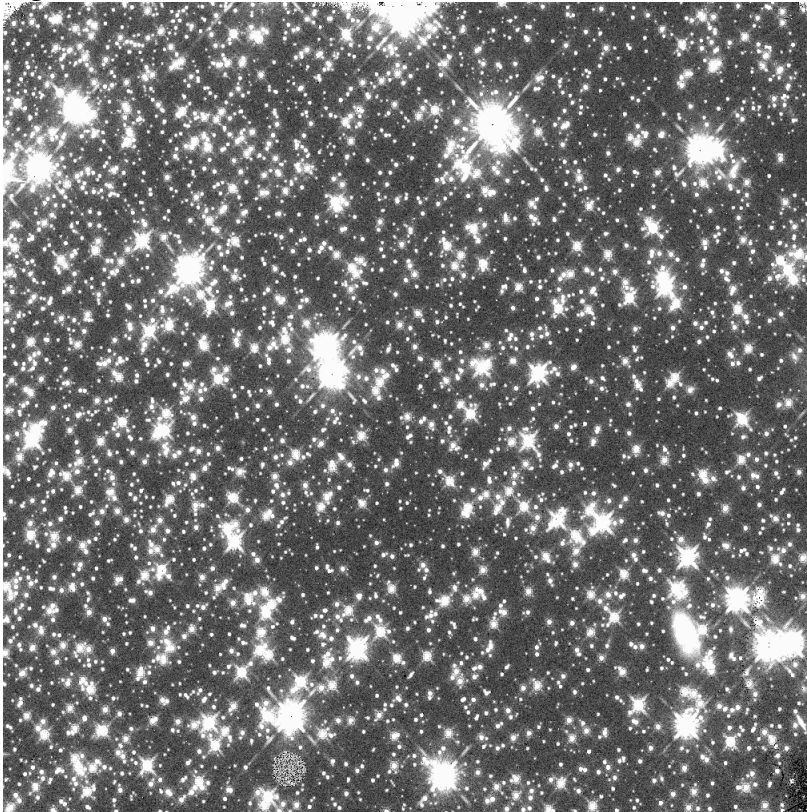
Algorithm

We want to determine if the corners of a pixel "see" a different flux for a star than the pixel's center. If we assume all pixels behave in the same way, then we can divide a representative pixel into a 5x5 grid of 25 "cells". Each cell represents the magnitude offset any star would experience if it landed in that cell as compared to the overall average of all possible positions (cells). From program 11916 we have images of Omega

Cen taken in a 4-point, subpixel dither pattern. For this data we can then set up a matrix of linear equations and solve for the unknowns, the values of the cells. To find the value for each cell, the (x,y) location of each star is converted to x mod 1, y mod 1, and all stars are plotted onto the representative pixel (Figure 3 shows the representative pixel with good coverage across the pixel). Each star then has six representative equations, where the magnitude differences between the four pointings are equal to the differences between the four populated cells. The program sets up the equations for all stars and solves using least squares fitting (see Appendix A). The result is a 5x5 image of the values of the 25 cells making up the representative pixel (see the Figures and Tables below).

Figure 3. X mod 1, Y mod 1 plotted on the representative pixel
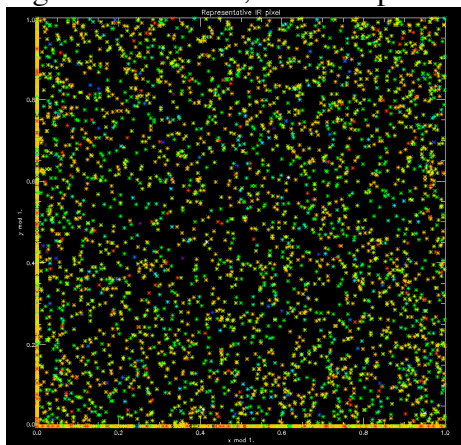
All Stars

In Table 3, the values in the cells represent the magnitude offset any star would experience if it lands in the corresponding cell compared to the overall average of all possible positions (cells). For example, in the case of the full frame F110W Omega Centauri image, if the star landed in the upper leftmost cell, the measured flux would be the average magnitude minus 0.0014. Likewise, if the star landed in the center cell, the measured flux would be the average magnitude plus 0.0067 (statistical analysis of these results are discussed in the following section).

Table 3. IPSV 5x5 solution for the full frame Omega Cen F110W filter

	-0.0014	0.0007	0.0009	0.0045	-0.0056
	-0.0019	0.0055	0.0048	-0.0005	-0.0046
	-0.0013	0.0120	0.0067	0.0034	0.0101
	0.0036	0.0064	0.0028	0.0038	-0.0001
	-0.0082	0.0031	-0.0005	-0.0047	-0.0070

Table 4. IPSV 5x5 solution for the full frame Omega Cen F160W filter

					-0.0021	0.0049	0.0143	0.0030	0.0063
					0.0018	0.0006	0.0014	-0.0017	0.0046
					-0.0014	-0.0027	-0.0071	-0.0023	0.0021
					-0.0004	-0.0008	0.0033	-0.0001	0.0060
					-0.0000	0.0084	0.0009	-0.0042	0.0024

Table 5. IPSV 5x5 solution for the full frame 47 Tuc F160W filter

					-0.0040	0.0049	0.0130	0.0150	-0.0088
					0.0073	0.0028	0.0077	0.0007	0.0093
					0.0021	0.0067	0.0114	0.0143	0.0066
					0.0009	0.0018	-0.0053	0.0008	-0.0031
					0.0016	0.0052	0.0040	-0.0021	-0.0036

In the following figure, we present the histogram of instrumental magnitudes for the stars in the F110W Omega Cen field. The histogram peaks at ~22.2 magnitudes. 37% of all the stars in the field are fainter than 22.0 magnitudes and approximately 50% of the stars are fainter than 21.5 magnitudes. Based on this histogram stars were grouped into three categories: fainter than 22.0 magnitudes, fainter than 21.5 magnitudes and brighter than 21.5 magnitudes. These designations were carried to the other fields even though their distributions were somewhat different (see Figures 4 – 6). We then repeated the all-star analysis on the subgroups (Tables 6 – 14).

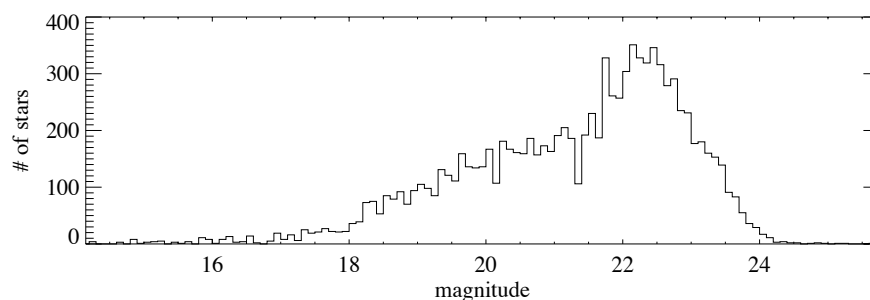Figure 4. Histogram of stars by magnitude in Omega Cen field in F110W

Figure 5. Histogram of stars by magnitude in Omega Cen field in F160W
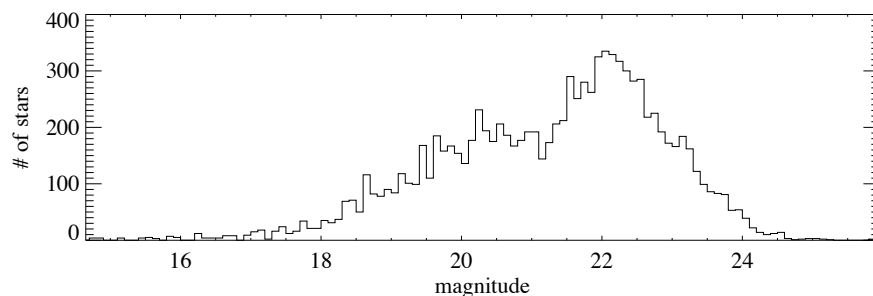
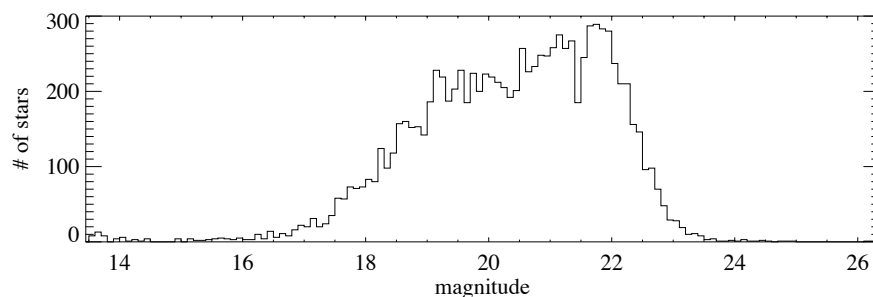Figure 6. Histogram of stars by magnitude in 47 Tuc field in F110W

Fainter than 21.5

Table 6. IPSV 5x5 solution for the full frame Omega Cen F110W filter

	-0.0014	-0.0006	0.0009	0.0092	-0.0107
	-0.0063	0.0078	0.0055	-0.0047	-0.0096
	-0.0076	0.0175	0.0085	0.0010	0.0174
	0.0077	0.0101	0.0039	0.0071	0.0010
	-0.0140	0.0020	-0.0031	-0.0100	-0.0122

Table 7. IPSV 5x5 solution for the full frame Omega Cen F160W filter

	-0.0050	0.0082	0.0264	-0.0026	0.0101
	0.0032	-0.0002	0.0023	-0.0057	0.0063
	-0.0067	-0.0065	-0.0120	-0.0046	0.0038
	-0.0018	-0.0038	0.0060	-0.0023	0.0104
	-0.0001	0.0135	0.0002	-0.0069	0.0034

Table 8. IPSV 5x5 solution for the full frame 47 Tuc F160W filter

	-0.0155	0.0044	0.0462	0.0340	-0.0379
	0.0191	-0.0062	-0.0002	-0.0153	0.0055
	0.0037	0.0137	-0.0010	0.0439	0.0234
	0.0056	-0.0095	-0.0320	0.0052	-0.0114
	0.0100	0.0208	-0.0040	-0.0256	-0.0029

Fainter than 22.0

Table 9. IPSV 5x5 solution for the full frame Omega Cen F110W filter

	-0.0004	-0.0049	-0.0001	0.0159	-0.0127
	-0.0064	0.0104	0.0062	-0.0069	-0.0109
	-0.0099	0.0181	0.0089	0.0024	0.0184
	0.0099	0.0120	0.0040	0.0093	0.0014
	-0.0141	0.0009	-0.0045	-0.0119	-0.0141

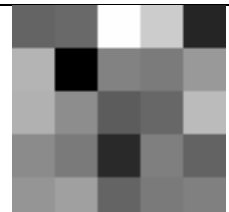Table 10. IPSV 5x5 solution for the full frame Omega Cen F160W filter

	-0.0106	0.0081	0.0320	-0.0035	0.0097
	0.0012	0.0002	0.0032	-0.0044	0.0054
	-0.0085	-0.0085	-0.0118	-0.0043	0.0064
	-0.0044	-0.0024	0.0089	-0.0035	0.0127
	0.0001	0.0162	0.0001	-0.0116	0.0043

Table 11. IPSV 5x5 solution for the full frame 47 Tuc F160W filter

	-0.0177	-0.0142	0.0998	0.0585	-0.0535
	0.0396	-0.0726	0.0030	-0.0019	0.0192
	0.0364	0.0101	-0.0223	-0.0153	0.0448
	0.0086	-0.0028	-0.0513	0.0005	-0.0179
	0.0165	0.0244	-0.0174	-0.0027	0.0011

Brighter than 21.5

Table 12. IPSV 5x5 solution for the full frame Omega Cen F110W filter

	-0.0042	0.0004	-0.0016	-0.0036	-0.0014
	0.0025	0.0022	0.0045	0.0036	0.0001
	0.0049	0.0030	0.0037	0.0058	-0.0003
	-0.0039	0.0007	-0.0009	-0.0012	-0.0035
	-0.0021	0.0031	0.0016	0.0006	-0.0017

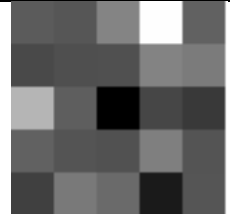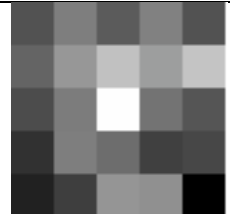Table 13. IPSV 5x5 solution for the full frame Omega Cen F160W filter

	-0.0003	-0.0005	0.0015	0.0076	-0.0001
	-0.0010	-0.0007	-0.0007	0.0014	0.0011
	0.0037	-0.0001	-0.0035	-0.0011	-0.0016
	-0.0001	-0.0006	-0.0007	0.0013	-0.0006
	-0.0013	0.0010	0.0003	-0.0026	-0.0005

Table 14. IPSV 5x5 solution for the full frame 47 Tuc F160W filter

	0.0000	0.0033	0.0007	0.0035	0.0001
	0.0013	0.0053	0.0090	0.0059	0.0092
	-0.0004	0.0031	0.0147	0.0024	0.0002
	-0.0022	0.0033	0.0020	-0.0012	-0.0008
	-0.0031	-0.0013	0.0052	0.0047	-0.0050

Results

Statistical analyses of the 5x5 IPSV solutions presented above are given in the following tables. For all of the IPSV solutions presented in this ISR we find that all the cell values fall within 3.0 standard deviations from the mean. No appreciable IPSV pattern appears across a pixel. Due to a lack of subpixel shifts, the 47 Tucanae data has a larger standard deviation then the Omega Centauri data.

Table 15. Summary of IPSV solution for all stars

image	# of stars	mean	stdev	min	max
Omega Cen F110W	**2533**	**0.00129**	**0.00507**	**-0.00824**	**0.01197**
Omega Cen F160W	**2579**	**0.00149**	**0.00442**	**-0.00711**	**0.01432**
47 Tuc F160W	2565	0.00357	0.00623	-0.00878	0.01500

Table 16. Summary of IPSV solution for stars fainter than 21.5 mag

image	# of stars	mean	stdev	min	max
Omega Cen F110W	**1356**	**0.00077**	**0.00879**	**-0.01405**	**0.01748**
Omega Cen F160W	**1319**	**0.00142**	**0.00820**	**-0.01202**	**0.02461**
47 Tuc F160W	697	0.00297	0.02104	-0.03790	0.04625

Table 17. Summary of IPSV solution for stars fainter than 22.0 mag

image	# of stars	mean	stdev	min	max
Omega Cen F110W	**1039**	**0.00084**	**0.01025**	**-0.01409**	**0.01837**
Omega Cen F160W	**963**	**0.00140**	**0.00992**	**-0.01184**	**0.03203**
47 Tuc F160W	347	0.00291	0.03659	-0.07264	0.09976

Table 18. Summary of IPSV solution for stars brighter then 21.5 mag

image	# of stars	mean	stdev	min	max
Omega Cen F110W	**1177**	**0.00049**	**0.00291**	**-0.00422**	**0.00583**
Omega Cen F160W	**1260**	**0.00007**	**0.00211**	**-0.00346**	**0.00759**
47 Tuc F160W	1868	0.00240	0.00433	-0.00505	0.01475

Intrapixel Capacitance

Intrapixel capacitance (IPC) is the deterministic crosstalk of charge in IR detectors like the WFC3 IR, where charge is spread into adjacent pixels before the pixels are read out. The IPC was modeled by Hilbert and McCullough (see ISR 2011-10) as a convolution with a small kernel and the effect was found to be small enough to not affect the photometry in the WFC3 IR detector. To confirm that IPC does not affect the IPSV results, a deconvolution program (McCullough, ISR 2011-10) was used to remove the IPC (using the parameters alpha=0.0175 and beta=0.0125) from the FLTs and the photometry was repeated. The IPSV analysis was performed on these IPC-corrected frames; the results were not significantly different from the previous IPSV runs, as shown in the tables below.

Table 19. Summary of IPSV solution for all stars, with IPC correction

image	# of stars	mean	stdev	min	max
Omega Cen F110W	2533	0.00129	0.00508	-0.00824	0.01197
Omega Cen F160W	2579	0.00149	0.00442	-0.00711	0.01432
47 Tuc F160W	2565	0.00357	0.00623	-0.00878	0.01500

Table 20. Summary of IPSV solution for stars fainter than 21.5 mag, with IPC correction

image	# of stars	mean	stdev	min	max
Omega Cen F110W	1356	0.00077	0.00880	-0.01405	0.01748
Omega Cen F160W	1319	0.00142	0.00820	-0.01202	0.02641
47 Tuc F160W	697	0.00297	0.02104	-0.03790	0.04625

Table 21. Summary of IPSV solution for stars fainter than 22.0 mag, with IPC correction

image	# of stars	mean	stdev	min	max
Omega Cen F110W	1039	0.00084	0.01025	-0.01409	0.01837
Omega Cen F160W	963	0.00140	0.00992	-0.01184	0.03203
47 Tuc F160W	347	0.00291	0.03659	-0.07264	0.09976

Table 22. Summary of IPSV solution for stars brighter then 21.5 mag, with IPC correction

image	# of stars	mean	stdev	min	max
Omega Cen F110W	1177	0.00050	0.00292	-0.00422	0.00583
Omega Cen F160W	1260	0.00008	0.00211	-0.00346	0.00759
47 Tuc F160W	1868	0.00240	0.004331	-0.00505	0.01475

Data by Amps

The data from Omega Cen F110W and F160W and 47 Tuc F160W were also analyzed as a function of amp. The results are shown in the following figures and tables. There is a larger standard deviation for these datasets due to the smaller number of stars, but the cell values still fall within 2.5 standard deviations from the mean and there are no patterns across the pixel.

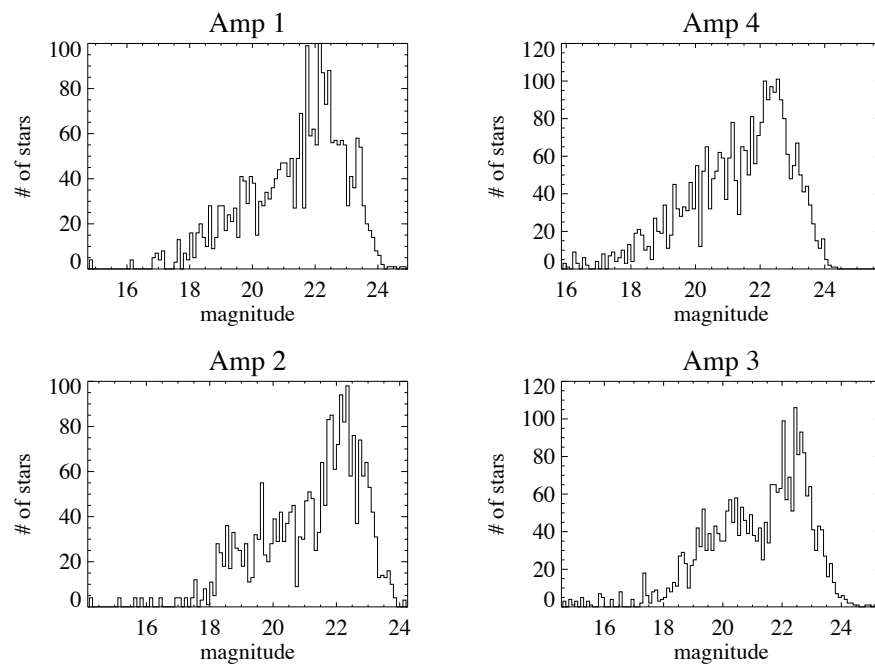Figure 7. Histogram of magnitudes for Omega Cen field F110W by Amp

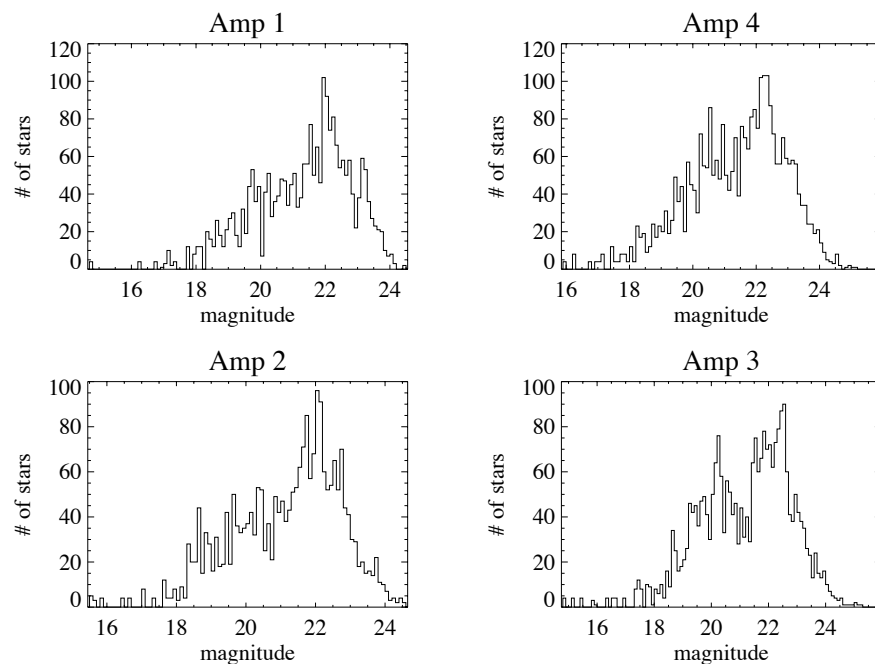Figure 8. Histogram of magnitudes for Omega Cen field F160W by Amp

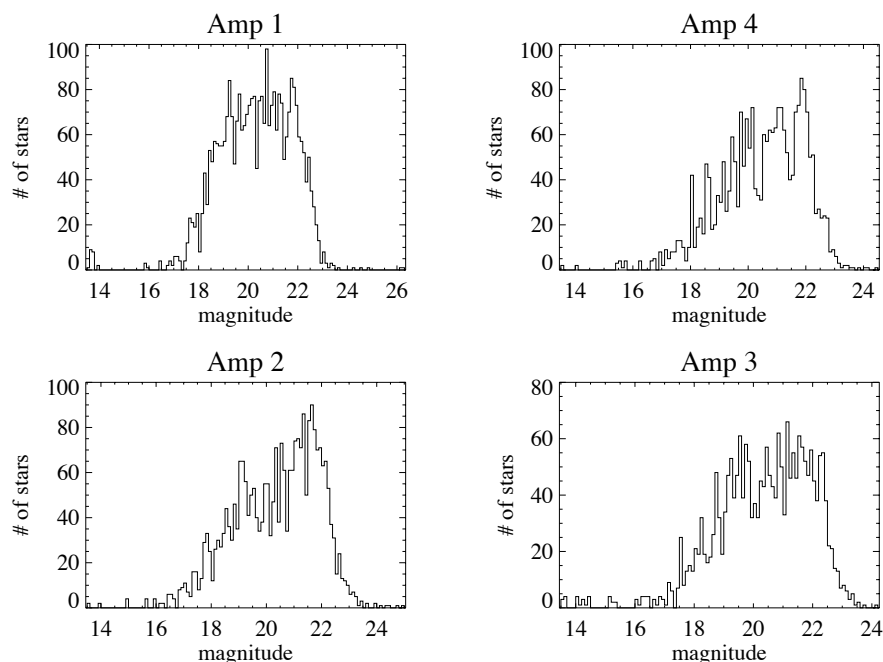Figure 9. Histogram of magnitudes for 47 Tuc field F160W by Amp

Table 23. Summary of IPSVsolution for each Amp

image	amp	# of stars	mean	stdev	min	max
Omega Cen F110W	A	593	0.00017	0.00506	-0.00815	0.00887
	B	708	-0.00018	0.01326	-0.01519	0.04787
	C	583	0.00081	0.00527	-0.00761	0.01220
	D	649	0.00006	0.00764	-0.01190	0.01224
Omega Cen F160W	A	592	0.0	0.00719	-0.01966	0.01453
	B	745	0.00004	0.00933	-0.01429	0.02328
	C	590	0.00009	0.00774	-0.01137	0.01932
	D	652	0.00004	0.00677	-0.01259	0.01816
47 Tuc F160W	A	765	0.00115	0.01612	-0.03891	0.03541
	B	588	0.00561	0.01076	-0.01434	0.03374
	C	667	-0.00049	0.01386	-0.02272	0.02361
	D	543	0.00031	0.01251	-0.02135	0.03002

Conclusions

This report summarizes the results of an on-orbit test for IPSV. With ~2500 stars and 4 dithers, there were ~50 times more stellar measurements in this test than in the TV3 experiment which, due to stimulus and time constraints, was limited to one point source and 200 dithers. Thus, the precision should be ~sqrt(50) = 7x greater precision, or ~0.1% measurement uncertainty of the IPSV. In our actual measurements for all stars in the Omega Centauri field, aperture photometry showed no dependence on the star's center,

13

with a standard deviation of 0.00507 and 0.00442 magnitudes, respectively for wavelengths of 1.1 and 1.6 microns, for differential photometric values (i.e., IPSV) represented on a regular grid of 5x5 elements spanning a nominal pixel of the WFC3 IR detector. To within that measurement error, and independent of wavelength, magnitude bin or amplifier we do not detect any IPSV.

References

Anderson, J. & King, I.R., 2009, High-Precision Astrometry with WFPC2. I. Deriving an Accurate Point-Spread Function, PASP, 112, 1360

Hilbert, B. & McCullough, P., ISR 2011-10: Interpixel Capacitance in the IR Channel: Measurements Made on Orbit, April 2011

Lauer, T., 1999, The Photometry of Undersampled Point-Spread Functions, PASP, 111, 1434

McCullough, P. & Bushouse, H., ISR 2008-29: WFC3 Testing: IR Intrapixel Sensitivity, December 2009

Appendix A

To solve for intrapixel sensitivity variance we start by dividing a representative pixel into 25 "cells". Using a 4-point subpixel dither pattern each star will fall into 4 different cells. Hopefully with rotations, distortions, and larger shifts all 25 cells will be connected, and we can solve for the intrapixel sensitivity.

A	B	C	D	E
F	G	H	I	J
K	L	M	N	O
P	Q	R	S	T
U	V	W	X	Y

Say a star lands in subpixel areas C,M,E & O. There are (25 choose 2) 300 distinct pairs, and associated with each pair is a flux ratio that does not depend on each star's unique and unknown brightness. A flux ratio is also a magnitude difference. So let A, B, C, … Y represent the magnitude offset any star would experience if it lands in the corresponding cell, compared to the overall average of all possible positions (cells).

We have ~2500 stars, each sampled 4 times (i.e. 4 subpixel dither positions) therefore for each star so we have (4 choose2) =6 differences in the value of the stars magnitude.

For star 1:
$$C-M=M_1(C) - M_1(M)$$
$$C-E=M_1(C) - M_1(E)$$
$$C-O=M_1(C) - M_1(O)$$
$$M-E=M_1(M) - M_1(E)$$
$$M-O=M_1(M) - M_1(O)$$
$$E-O=M_1(E) - M_1(O)$$

So we have a matrix (linear) equation: $Z \bullet V = \Delta M_i$ where V is a vector of parameters (A,B,C,…Y) and Z is a sparse matrix of +1's and -1's corresponding to all the equations LHS and ΔM_i is the vector of the RHS of those same equations. Z is 25xn elements, mostly zeros, with n=number of unique differential photometric measurements of stars. We used standard procedures to solve for V by least squares or SVD. We validated the algorithm on simulated photometric data with a known IPSV superposed.